Impact of Electrode Geometry on the Efficiency of Metal–Semiconductor–Metal AlGaN Ultraviolet Photodiodes

S. F. Nwabunwanne and W. R. Donaldson

Laboratory for Laser Energetics, University of Rochester

Fast aluminum-gallium-nitride ($Al_xGa_{1-x}N$)–based metal–semiconductor–metal (MSM) ultraviolet (UV) photodiodes (PD's) have been successfully designed, fabricated, and characterized using conventional photolithography techniques. Various electrode geometries were fabricated to investigate the influence of metal contact shapes on device performance indices with emphasis on the response speed and bias-voltage–independent efficiency. Peak response times from the best devices were evaluated with a bias-voltage–independent, external quantum efficiency of 1198% at 19.5 V and 70% at 60 V for *n*-doped and intrinsic devices, respectively. Based on the measured mobility, these devices should be capable of a response time as short as 1.31 ps.

$Al_xGa_{1-x}N$-based UV PD's have been the subject of active research due to their intriguing material properties. Sustained interest in $Al_xGa_{1-x}N$ photodetectors stems from their impressive characteristics such as a wide and tunable direct band gap, thermal resistivity, radiation sturdiness, and electrical robustness. The ability to easily select the detected wavelength by simply varying the aluminum content of $Al_xGa_{1-x}N$ is a significant advantage of these group III–V compounds. Also, $Al_xGa_{1-x}N$ photodetectors can be specifically designed to look at specific spectral windows.[1,2]

Intrinsic and Si-doped wafers obtained from KYMA Technologies were prepared by metal organic chemical-vapor deposition (MOCVD). A thin AlN layer serves to minimize the lattice constant mismatch between intrinsic/*n*-doped AlGaN thin films and the sapphire substrate. Si-doped wafers have a carrier density of 1×10^{18} cm^{-3}, while the intrinsic wafers have a carrier density of 1×10^{17} cm^{-3}. The Hall-effect measurements of Si-doped $Al_{0.1}Ga_{0.9}N$ thin films using the van der Pauw[3] geometry configuration resulted in a carrier mobility of 127 cm^{2}V^{-1}s^{-1}, a carrier density of 2×10^{18} cm^{-3}, and a resistivity of 0.0243 Ωcm. Similarly, for Si-doped $Al_{0.2}Ga_{0.8}N$ thin film, the carrier mobility was measured as 10.4 cm^{2}V^{-1}s^{-1}, the carrier density as 1×10^{18} cm^{-3}, and resistivity as 0.5656 Ωcm. We investigated the defect densities of the wafers using x-ray rocking-curve measurements, which yielded 1.4398×10^6 cm^{-2} and 1.9288×10^6 cm^{-2} dislocation densities for intrinsic $Al_{0.1}Ga_{0.9}N$ and $Al_{0.2}Ga_{0.8}N$ thin films, respectively. For *n*-doped wafers, dislocation densities were 1.0201×10^6 cm^{-2} and 1.4702×10^6 cm^{-2} for $Al_{0.1}Ga_{0.9}N$ and $Al_{0.3}Ga_{0.7}N$, respectively. These numbers are among the lowest reported dislocation densities in AlGaN thin films; typically dislocation densities are of the order of 10^7 to 10^8 cm^{-2} (Refs. 2 and 4).

Two different electrode geometries were fabricated on the Pt and Au devices. There are a total of five interdigitated fingers for each device configuration, which consists of 1×5-μm-wide electrodes that are spaced at 2-μm and 3-μm intervals. The electrodes on our previous devices covered 50% (Ref. 1) of the active area but these devices' electrodes cover about 30% of the active area. This implies ~20%-more incident UV light will be absorbed by the PD, resulting in improved sensitivity. An antireflection (AR) layer consisting of 44 nm of SiO_2 was designed for near-zero reflectivity at 262 nm, contributing ~20% improvement in the external quantum efficiency (EQE) of the PD's.

The light source was a 262-nm *Q*-switched Crystalaser with 10-ns pulse duration and 4.5 nJ of energy, externally clocked at 2.5 kHz. The beam diameter of the laser at the PD was 138 μm. Approximately 0.05 nJ per pulse reached the active area of the device. A Si-biased PD was employed as a reference detector to account for variation in the pulse energy. A half-wave plate combined with the UV polarizer was employed to control the amount of UV energy reaching both diodes during the reference

diode calibration. A 12.5-GHz Tektronix oscilloscope served as the primary measurement tool for the MSM AlGaN PD's, which introduced a bandwidth constraint on our ability to measure the intrinsic impulse response of these devices.

With the electrode's geometry varied to facilitate absorption of 20% more of the incident photons as well as a strong electric field of 1×10^7 V/m at 20-V bias voltage, which is 40% greater than the electric field in the previous devices, we observed for the first time with these PD's, a bias-voltage–independent EQE of 1198% at 19.5 V and 70% at 60 V for the best-performing *n*-doped and intrinsic devices, respectively. As evidenced by the long tail in response, the Pt device must be in photoconductive mode, causing a multiplication of carriers that accounts for the superhigh EQE. While we desire efficient devices, the photoconductive gains of some of these devices are unsuitable for ultrafast laser pulse characterization due to their long tails. The EQE of the AlGaN devices, which is the ratio of the number of photogenerated carriers to the number of incident photons, was calculated using

$$QE(\eta) = \frac{I_{\text{ph}}/e}{P/h\nu}, \tag{1}$$

where I_{ph} is the photocurrent (A) obtained by averaging the diode's voltage response measured over time and multiple acquisitions and dividing by 50-Ω oscilloscope's impedance; e is the charge; P denotes the optical power (W) of the incident light; h is Planck's constant; and ν is the frequency (Hz) of the input light. The voltage response curves were acquired ten times at each bias voltage and then integrated over 1.5-ns time interval. The efficiency of a PD is shown in Fig. 1. This represents a significant improvement over previous devices. A plausible contribution to the improvement in the EQE is the elevated electric field that drove the photogenerated carriers to saturation velocity, thereby preventing their recombination before they could be removed at the contacts. We estimate that the elevated electric field contributed about 30% to the boost in the EQE. Furthermore, the low number of defects in the $Al_xGa_{1-x}N$ thin films translated to a reduced number of trap sites that impede the free flow of carriers when photoexcited. This improved the mobility of the carriers, leading to a pronounced 30% increase in the EQE. Finally, the Schottky contacts formed with Pt and Au have been reported to reduce UV detection since they cast opaque shadows on the semiconductor, thereby reducing the efficiency of UV absorption.[5–7] We reduce this impact of Pt and Au electrodes by making them thinner and fewer in number. Also, Schottky contacts block current from –5 V to 5 V, which is less than –8 V to 8 V in the previous devices, thereby leading to a rise in the photocurrent and contributing ~20% to the jump in the EQE. Finally, it is evident that some photoconductive gain mechanisms could have added to the photogenerated current accounting for about 10% elevation in the EQE for intrinsic devices and adding >50% in *n*-doped devices.

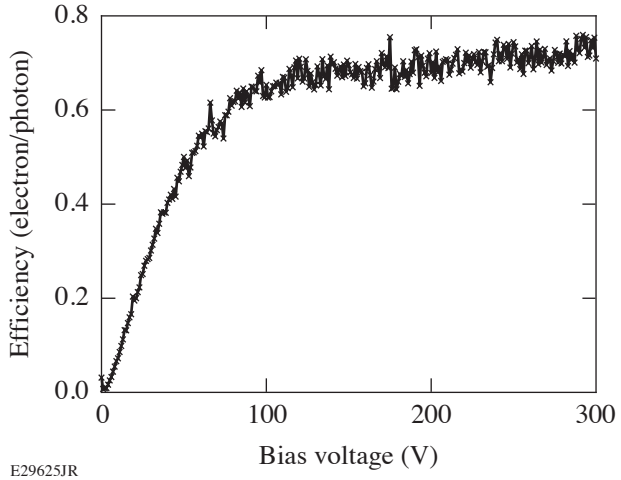

Figure 1
External quantum efficiency of AlGaN PD as a function of bias voltage with saturation beginning at 75 V.

This material is based upon work supported by the Department of Energy National Nuclear Security Administration under Award Number DE-NA0003856, the University of Rochester, and the New York State Energy Research and Development Authority.

1. Y. Zhao and W. R. Donaldson, IEEE J. Quantum Electron. **56**, 4000607 (2020).
2. Y. Zhao and W. R. Donaldson, IEEE Trans. Electron Devices **65**, 4441 (2018).
3. D. M. Boerger, J. J. Kramer, and L. D. Partain, J. Appl. Phys. **52**, 269 (1981).
4. R. Gaska *et al.*, Appl. Phys. Lett. **72**, 707 (1998).
5. S. Wang *et al.*, IEEE Photon. Technol. Lett. **33**, 213 (2021).
6. P. C. Chang *et al.*, J. Alloys Compd. **504**, S429 (2010).
7. F. Bouzid, L. Dehimi, and F. Pezzimenti, J. Electron. Mater. **46**, 6563 (2017).